Charge-density-wave order parameter of the Falicov-Kimball model in infinite dimensions

Ling Chen* and J. K. Freericks†
Department of Physics, Georgetown University, Washington, DC 20057, USA

B. A. Jones‡
IBM, Almaden Research Center, 650 Harry Rd., San Jose, California 95120, USA

(Received 16 June 2003; published 15 October 2003)

In the large-U limit, the Falicov-Kimball model maps onto an effective Ising model, with an order parameter described by a BCS-like mean-field theory in infinite dimensions. In the small-U limit, van Dongen and Vollhardt showed that the order parameter assumes a strange non-BCS-like shape with a sharp reduction near $T \approx T_c/2$. Here we numerically investigate the crossover between these two regimes and qualitatively determine the order parameter for a variety of different values of U. We find the overall behavior of the order parameter as a function of temperature to be quite anomalous.

DOI: 10.1103/PhysRevB.68.153102 PACS number(s): 71.10.−w, 71.30.+h, 71.45.−d, 72.10.−d

Dynamical mean-field theory[1] has been widely used to study electron correlations in a variety of different interacting systems. Much work has focused on the ''paramagnetic'' metal-insulator transition, on transport properties in the normal state, and on determining phase diagrams to ordered phases via a susceptibility analysis or a Maxwell construction. The properties of the ordered phase have been less studied, yet there is much interesting physics to examine there. For example, one might have thought that since the system is infinite dimensional, both the critical behavior and the order parameter as a function of temperature would be determined by a BCS-like mean-field picture. Indeed, the critical exponents are always mean-field like, but the order parameter can have quite anomalous behavior as a function of temperature. This anomalous behavior is amplified for small correlation strength, since many models map onto effective spin models for large correlations, and the order parameter of an infinite-dimensional spin model is always mean-field-like. In this contribution, we examine in detail the case of a commensurate (two-sublattice) charge-density-wave (CDW) phase in the spinless Falicov-Kimball model at half filling. Analytical work in the large and small-U limits has already been carried out.[2,3]

The Falicov Kimball (FK) model[4] was introduced in 1969 to describe metal-insulator transitions in transition-metal and rare-earth compounds. The model consists of two types of particles: itinerant conduction electrons and localized ions that mutually interact with an on-site Coulomb interaction. It is the simplest Fermionic model of electron correlations and the spinless version can be interpreted as a simple model for crystallization,[5] where the system has a phase transition from a disordered phase at high temperature to an ordered phase as the temperature is lowered. We examine the order parameter as a function of temperature here.

Many-body effects enter via the statistical mechanics associated with annealed averaging. The FK model is the simplest many-body problem that can be solved exactly in the limit of large dimensions. Brandt and Mielsch[6–8] presented the first solution of this problem using dynamical mean-field theory. Their solution quantitatively illustrated how a period-two CDW phase is stabilized at low temperatures.

For the symmetric half filled case on a bipartite lattice, the ordering is into a commensurate CDW state, in which the particles order in a checkerboard pattern: the conduction electrons preferentially occupy one sublattice, and the ions the other one. van Dongen and Vollhardt[2,3] derived an analytical expression for the critical temperature T_c as a function of the Coulomb interaction in the large and small-U limits. For large U, it has the conventional strong-coupling t^2/U form, but for small coupling, T_c is much larger than the BCS-like exponential form of $\exp[-C/U]$. They obtained similar results for the order parameter—for large U it behaved mean-field like, but for small U the behavior was quite anomalous with a sharp decrease as $T \to T_c/2$. Here we numerically explore the behavior of the order parameter between these two limits. A self-consistent algorithm[9] is employed to perform efficient computations at low temperature and to make it feasible to study the order parameter when U is small. Surprisingly, the order parameter is not BCS like!

The spinless Falicov-Kimball model is represented by the following Hamiltonian:

$$\mathcal{H} = -\sum_{ij} t_{ij} c_i^\dagger c_j + E_f \sum_i f_i^\dagger f_i + U \sum_i c_i^\dagger c_i f_i^\dagger f_i . \qquad (1)$$

The conduction electrons (created or destroyed at site i by $c_i^\dagger$ or c_i) can hop between nearest-neighbor sites with a hopping matrix[1] $-t_{ij} = -t^*/2\sqrt{D}$. The localized ions (created or destroyed at site i by $f_i^\dagger$ or f_i) have a site energy E_f. There is a Coulomb interaction U between the localized ions and the conduction electrons that sit at the same lattice site. A chemical potential μ is employed to determine the number of conduction electrons. At half filling, we have $\mu = U/2$ and $E_f = -U/2$.

We examine two bipartite lattices here—the hypercubic lattice with a density of states (DOS) given by $\rho(\epsilon) = \exp(-\epsilon^2)/t^*\sqrt{\pi}$ and the infinite-coordination Bethe lattice with $\rho(\epsilon) = \sqrt{4-\epsilon^2}/t^* 2\pi$ (we take $t^* = 1$ as our energy unit). The local Green's function $G(i\omega_n)$ can be written as the Hilbert transform of the noninteracting DOS $\rho(\epsilon)$,

$$G(i\omega_n)=\int d\epsilon\rho(\epsilon)\frac{1}{i\omega_n+\mu-\Sigma_n-\epsilon}, \tag{2}$$

where $\omega_n=\pi T(2n+1)$ is the Fermionic Matsubara frequency and $\Sigma(i\omega_n)=\Sigma_n$ is the local self-energy. Dyson's equation for the local self-energy reads

$$\Sigma_n=i\omega_n+\mu-\lambda_n-G^{-1}(i\omega_n) \tag{3}$$

with λ_n the dynamical mean field evaluated at the nth Matsubara frequency. The effective medium Green's function $G_0(i\omega_n)$ is

$$G_0(i\omega_n)=\frac{1}{G^{-1}(i\omega_n)+\Sigma_n}=\frac{1}{i\omega_n+\mu-\lambda_n}. \tag{4}$$

Solving the atomic problem in a time-dependent field yields another equation for the local Green's function,

$$G(i\omega_n)=\frac{1-w_1}{i\omega_n+\mu-\lambda_n}+\frac{w_1}{i\omega_n+\mu-\lambda_n-U}, \tag{5}$$

where w_1 represents the density of the ions which is determined by the atomic partition function

$$\mathcal{Z}_{at}(\lambda)=\mathcal{Z}_0(\lambda,\mu)+e^{-\beta E_f}\mathcal{Z}_0(\lambda,\mu-U) \tag{6}$$

with

$$\mathcal{Z}_0(\lambda,\mu)=2e^{\beta\mu/2}\prod_n\frac{i\omega_n+\mu-\lambda_n}{i\omega_n} \tag{7}$$

and $w_1=e^{-\beta E_f}\mathcal{Z}_0(\lambda,\mu-U)/\mathcal{Z}_{at}$. When $E_f=-U/2$ and $\mu=U/2$, then λ_n is pure imaginary and we have $w_1=0.5$.

The iterative algorithm for finding the self-energy is that of Jarrell:[10] (i) first set the self-energy equal to zero; (ii) then determine the local Green's function from Eq. (2); (iii) then determine the effective-medium Green's function from Eq. (4) and the ion density from the atomic partition function (in our case we always have $w_1=0.5$); (iv) next determine the new local Green's function from Eq. (5) and the new self-energy from Eq. (3). Starting with the new self-energy, repeat steps (ii)–(iv) until convergence is reached.

After solving for the self-energy and the Green's functions, the susceptibility to a CDW instability ($T\chi=\langle n_i n_j\rangle-\langle n_i\rangle\langle n_j\rangle$) can be calculated following the derivation of Brandt and Mielsch.[6,7] At high temperature, the electrons are uniformly distributed throughout the lattice. As the temperature is lowered, the charge density becomes nonuniform when the momentum-dependent susceptibility diverges and a CDW forms. After some tedious algebra, the transition temperature is found to occur when

$$1=\sum_n\frac{w_1(1-w_1)U^2G_n^3\eta_n(q)}{(1+G_n\Sigma_n)[1+G_n(\Sigma_n-U)]}\times\frac{1}{1+G_n[\Sigma_n-(1-w_1)U]+G_n\eta_n(q)[1+G_n(2\Sigma_n-U)]} \tag{8}$$

holds, where

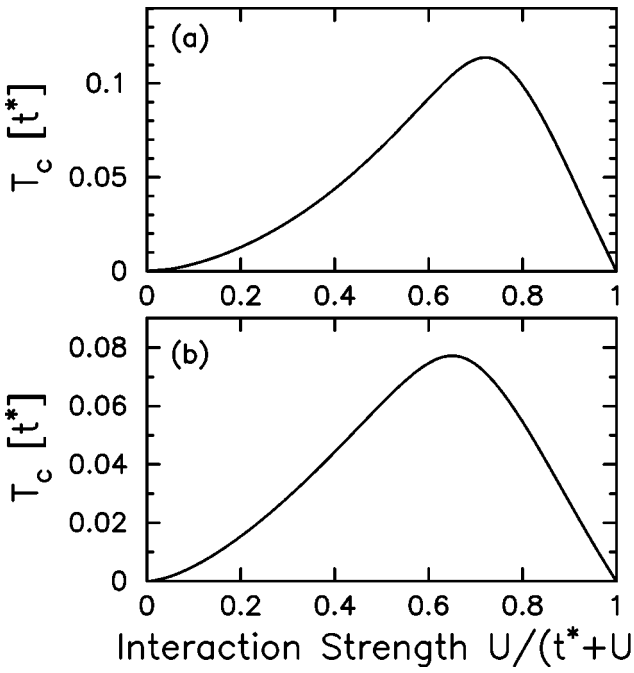

FIG. 1. Transition temperature for the ($X=-1$) CDW at half filling on (a) the Bethe lattice and (b) the hypercubic lattice as determined from the solution of Eq. (8). The horizontal axis is plotted as $U/(t^*+U)$ in order to include both the weak- and strong-coupling results on the same graph.

$$\eta_n(q)=-\frac{G_n}{\tilde{\chi}_n^0(q)}-G_n^{-1} \tag{9}$$

and the bare susceptibility satisfies

$$\tilde{\chi}_n^0(q)=-\frac{1}{N}\sum_q G_n(k+q)G_n(q) \tag{10}$$

in terms of the momentum-dependent Green's functions (N is the number of lattice sites). The q dependence of χ can be summarized by the scalar parameter[11]

$$X(q)=\lim_{D\to\infty}\frac{1}{D}\sum_{i=1}^{D}\cos q_i. \tag{11}$$

For $X=-1$, there is a phase transition from a uniform distribution to a (two-sublattice) checkerboard phase when the temperature falls below T_c. This transition temperature is plotted versus U for (a) the Bethe lattice and (b) the hypercubic lattice in Fig. 1.

For $T<T_c$, we need to revise the algorithm to solve for the Green's functions and to determine the order parameter. Since the thermodynamic quantities now differ on the A and B sublattices of the bipartite lattice, we label them by their respective sublattice. The order parameter for the CDW is defined to be $\Delta=|w_1^A-w_1^B|$. We find that if we try to iterate a generalization of the Jarrell algorithm to include the possibility of CDW order, then the equations suffer from ''critical slowing down'' as one approaches T_c from below. This would make an efficient determination of the order param-

eter as a function of T impossible when T_c became small because the number of Matsubara frequencies employed becomes large, and the equations must be iterated for a long time to achieve convergence. Instead, we adopt a variant of the algorithm proposed by Gruber *et al.*[9] We start by setting the self-energies on each sublattice to zero. Then we (i) choose a value for the order parameter $0<\Delta<1$ and set $w_1^A=0.5(1+\Delta)$ and $w_1^B=0.5(1-\Delta)$; (ii) we determine the parameter Z_n defined by

$$Z_n=\sqrt{(i\omega_n+\mu-\Sigma_n^A)(i\omega_n+\mu-\Sigma_n^B)} \tag{12}$$

and calculate the local Green's function on the A sublattice,

$$G_n^A=\frac{i\omega_n+\mu-\Sigma_n^B}{Z_n}\int d\epsilon\frac{\rho(\epsilon)}{Z_n-\epsilon}; \tag{13}$$

(iii) we solve for the effective medium on the A sublattice,

$$G_0^A(i\omega_n)=(G_n^{A-1}+\Sigma_n^A)^{-1}; \tag{14}$$

and (iv) we calculate the new local Green's function,

$$G_n^A=(1-w_1^A)G_0^A(i\omega_n)+\frac{w_1^A}{G_0^{A-1}(i\omega_n)-U}; \tag{15}$$

finally (v) we determine the new self-energy,

$$\Sigma_n^A=G_0^{A-1}(i\omega_n)-G_n^{A-1}. \tag{16}$$

Next we perform a similar analysis on the B sublattice: (vi) first we update Z_n then calculate the local Green's function on the B sublattice,

$$G_n^B=\frac{i\omega_n+\mu-\Sigma_n^A}{Z_n}\int d\epsilon\frac{\rho(\epsilon)}{Z_n-\epsilon}; \tag{17}$$

(vii) we determine the effective medium,

$$G_0^B(i\omega_n)=(G_n^{B-1}+\Sigma_n^B)^{-1}; \tag{18}$$

and (viii) we find the new local Green's function,

$$G_n^B=(1-w_1^B)G_0^B(i\omega_n)+\frac{w_1^B}{G_0^{B-1}(i\omega_n)-U}; \tag{19}$$

finally (ix) we calculate the new self-energy,

$$\Sigma_n^B=G_0^{B-1}(i\omega_n)-G_n^{B-1}. \tag{20}$$

Steps (ii)–(ix) are repeated until converged. Then we (*x*) calculate the local ion site energy on each sublattice by solving the generalization of the formula for the filling w_1 to the two-sublattice case, and solving for the E_f on each sublattice,

$$E_f^A=\frac{U}{2}+T\ln\left[\frac{1-w_1^A}{w_1^A}\right]+T\sum_n \ln[1-UG_0^A(i\omega_n)], \tag{21}$$

and

$$E_f^B=\frac{U}{2}+T\ln\left[\frac{1-w_1^B}{w_1^B}\right]+T\sum_n \ln[1-UG_0^B(i\omega_n)]. \tag{22}$$

If $E_f^A=E_f^B$, then a consistent thermodynamic solution has been achieved. If not, then we adjust the order parameter Δ and repeat the algorithm starting at step (i) until a consistent solution is reached. Since the ion densities on each sublattice are not updated during the iterative part of the algorithm, this technique does not suffer from critical slowing down, and it is easy to perform on both the Bethe lattice and the hypercubic lattice, simply by changing the corresponding DOS in the Hilbert transforms of Eqs. (13) and (17). In our numerical calculations, we use an energy cutoff of $10t^*$ for the Matsubara frequencies; the maximum number of Matsubara frequencies we include is 250 000.

For $U\to\infty$, the FK model maps onto an antiferromagnetic Ising model with $J=t^{*2}/4DU$. This spin system can be analyzed with static mean-field theory to yield the order parameter in a Curie-Weiss form,

$$\Delta=\tanh\left(\frac{\Delta T_c}{T}\right), \tag{23}$$

with $T_c=t^{*2}/4U$ on the hypercubic lattice. For $U\to 0$, the order parameter varies sharply from this result, with a steep decrease near $T_c/2$ and a flattening out before going to zero at T_c (note that at $U=0$ there is no T_c and the order parameter vanishes, but for any nonzero U, there is a transition, and one can examine the behavior of the order parameter, as we do here). We examine the transition between these two limits numerically. We find that U must be very small to even see the deviations from the mean-field theory curve. The evolution from the small-U to large-U limits is nonmonotonic. As U increases, the order parameter curve becomes steeper and steeper near T_c and flatter and flatter for small T until we reach the U corresponding to approximately the maximum of the T_c versus U curve. Once U increases past the maximum, then the order parameter curve slowly approaches the large-U limit.

We illustrate this behavior in Fig. 2 for the Bethe lattice. When U lies below 0.2 [panel (a)], we can see the depression in the curve develop as we evolve toward the $U=0$ limit. For $0.2<U<2.6$, the curve moves to the right and becomes steeper (but the critical exponent always remains 0.5) [panel (b)]. Finally, for larger values of U, the curve moves to the left until it assumes the mean-field-theory form [panel (c)].

The results on the hypercubic lattice are similar and are shown in Fig. 3. We show only two different regimes, as the curve is steepest when U lies near 1.0. Note that there are no analytic results available for the $U\to 0$ limit on the hypercubic lattice. The one difference from the Bethe lattice, is that here, the curves move to the left as we increase from $U=1$ to $U=4$, but they overshoot the mean-field theory curve, so they move back to the right to reach the $U\to\infty$ limit for larger values of U.

In summary, we have shown that the order parameter has an anomalous evolution as a function of temperature for small U in the spinless FK model. One can ask is this anoma-

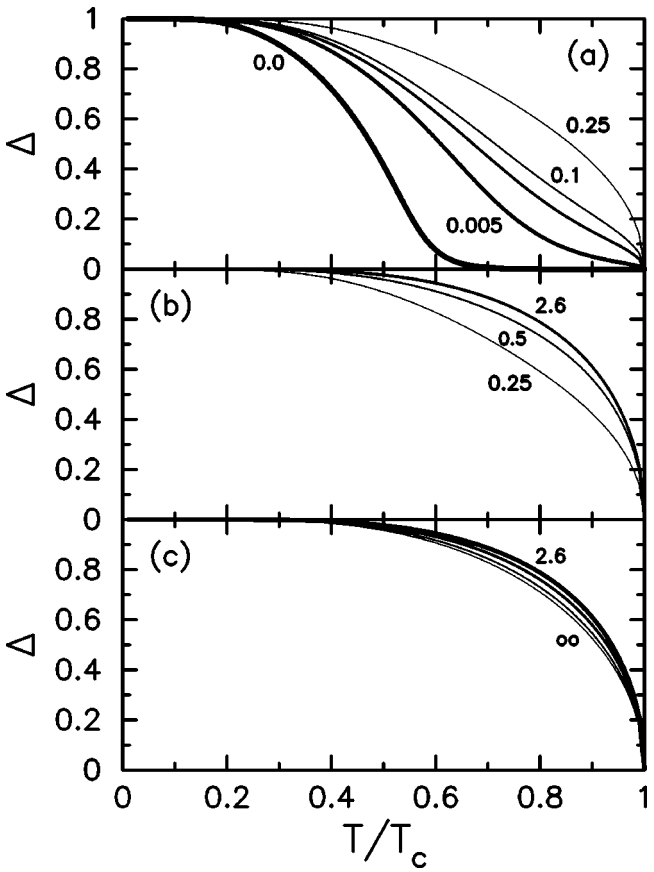

FIG. 2. Order parameter for the ($X=-1$) CDW of the FK model at half filling on the Bethe lattice. Panel (a) shows the small-U results where a depression can be seen ($U\rightarrow 0$, 0.005, 0.03, 0.1, and 0.25), panel (b) shows the intermediate results ($U=0.25$, 0.5, and 2.6), where the order-parameter curve moves out to the right as U is increased, and panel (c) shows the large-U regime ($U=2.6$, 3.0, 4.0, and ∞), where the curve shifts to the left and ultimately takes the mean-field-theory form.

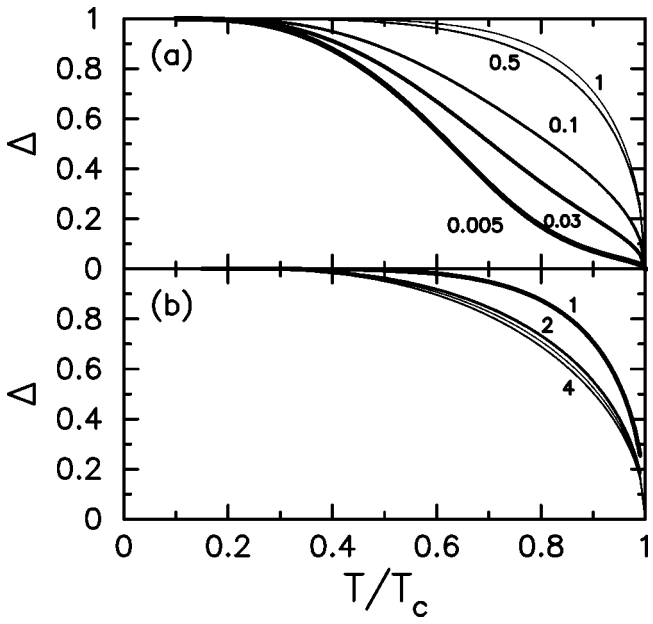

FIG. 3. Order parameter for the ($X=-1$) CDW of the FK model at half filling on the hypercubic lattice. Panel (a) shows the small-U results where a depression can be seen ($U=0.005$, 0.03, 0.1, 0.5, and 1.0) and panel (b) shows the larger-U results ($U=1.0$, 2.0, 4.0, and ∞), where the order parameter curve moves back to the left as U is increased, but overshoots, and then moves to the right to ultimately take the mean-field-theory form (which is the curve lying in between the $U=2$ and $U=4$ results).

lous behavior something generic to many-body systems, to the infinite-dimensional limit, or to the FK model. We tend to believe that it is most likely a curious property of the FK model itself. The weak-coupling limit of the FK model is known to have anomalous behavior for its T_c, being much higher than what would be predicted by a BCS approach, and it is possible that the anomalous shape survives in finite dimensions as well. Unfortunately, our numerical calculations show that U must be very small in order to see the anomalous shape emerge, and it is likely that the T_c is so small, that numerical calculations in finite dimensions may have trouble being performed at the temperatures necessary to see the anomaly. Even in infinite dimensions, we are limited by how small we can make U because the T_c is pushed so low that the number of Matsubara frequencies included in the calculation grows too large.

We acknowledge support from the National Science Foundation under Grant No. DMR-0210717. L.C. would like to thank the IBM Almaden Research Center for hosting him as a visitor while this work was completed.

*Electronic address: lc63@georgetown.edu
†Electronic address: freericks@physics.georgetown.edu; URL: http://www.physics.georgetown.edu/~jkf
‡Electronic address: bajones@almaden.ibm.com

[1] W. Metzner and D. Vollhardt, Phys. Rev. Lett. **62**, 324 (1989).
[2] P.G.J. van Dongen and D. Vollhardt, Phys. Rev. Lett. **65**, 1663 (1990).
[3] P.G.J. van Dongen, Phys. Rev. B **45**, 2267 (1992).
[4] L.M. Falicov and J.C. Kimball, Phys. Rev. Lett. **22**, 997 (1969).
[5] T. Kennedy and E. Lieb, Physica A **138**, 320 (1986).
[6] U. Brandt and C. Mielsch, Z. Phys. B: Condens. Matter **75**, 365 (1989).
[7] U. Brandt and C. Mielsch, Z. Phys. B: Condens. Matter **79**, 295 (1990).
[8] U. Brandt and C. Mielsch, Z. Phys. B: Condens. Matter **82**, 37 (1991).
[9] C. Gruber, N. Macris, P. Royer, and J.K. Freericks, Phys. Rev. B **63**, 165111 (2001).
[10] M. Jarrell, Phys. Rev. Lett. **69**, 168 (1992).
[11] E. Müller-Hartmann, Z. Phys. B: Condens. Matter **76**, 211 (1989).